Investigation of Material Models for Laser Welds in Crash Applications using LS-DYNA

N. Kuppuswamy [1], F. Seeger [1], M. Feucht [1], R. Schmidt [2]

[1] DaimlerChrysler AG, Germany

[2] Institute of General Mechanics, RWTH Aachen University, Germany

Abstract:

In general the body-in-white (BIW) consists of thin walled structures joined with adhesives, spot welds, laser welds etc. Due to the efficiency and reliability of laser welding, it is increasingly applied in automotive applications to join structures made of steel. The analysis of the behavior of all these joining technologies at crash is generally of great interest. Therefore a suitable model for spot welds has been already published by DaimlerChrysler AG at the LS-DYNA Forum 2005 [2]. Although there are a lot of similarities between laser welds and spot welds, new models and methods are required due to different weld properties and numerous possible laser weld geometries. Because the crash model of a BIW target structure consists of a relatively coarse mesh, a simplified model with reduced complexity is needed. Besides the modeling technique, the material model determines the quality and the efficiency of the modeled laser weld and BIW model. In this paper three different material models are investigated: a bi-linear elasto-plastic material (MAT100), a linear elastic visco-plastic material (MAT24) and a new linear elastic material with an anisotropic yield surface according to Hill, visco-plasticity and anisotropic damage according to Chaboche together with a failure criterion are compared. These material models are tested on standard substitute joint models with a single weld, where the weld has been modeled with a solid element.

Keywords:

Laser welding, crash, coarse finite element meshes, substitute joint models, material models, Chaboche, Hill, damage, failure criteria

1 Introduction

There are a number of commercially available finite element (FE) packages used to solve the problems related to crash applications. Most of the FE software contain very robust and well suited material models for steel, aluminum, rubber etc. These material models cover most of the general applications but they are not tailor-made to suit certain specific problems. One such industry related problem which will be discussed at length in this paper is the material modeling and analysis of laser welds in crash applications using LS-DYNA FE software.

In a crash application, the failure of the weld and its surroundings is a complex process. To reproduce the complete phase from the point of loading to the tear or failure of the weld, a suitable material model should encompass the following phases, viz. elasticity, non-linear plasticity with strain rate effects, non-linear damage followed by failure. The material model should also be applicable to different modeling techniques or geometry of the weld or the type of element chosen [1]. Known material models in LS-DYNA, viz. Mat 24, which is a linear elastic and non-linear plastic model with strain rate effects, and Mat100, a prominently used bi-linear elasto-plastic model for spot welds, are considered for this application. Apart from the above mentioned material models, a new phenomenological material model is developed and tested.

The new material model has been developed with an intention to answer problems related to steel and laser welded joints in particular. There are different formulations available to describe the yield surface of a material. Some of the well known and also commonly used yield conditions [8] are those of von Mises, Tresca, Hill, Drucker-Prager, Tsai etc. There are different theories related to post-elastic behavior describing the hardening and strain rate effects. Simple linear kinematic hardening models to non-linear kinematic or isotropic hardening models are also available. One such non-linear hardening model along with strain rate effects which is widely used is the model according to Chaboche combined with von Mises plasticity [3]. There are also different kinds of damage models available with isotropic and anisotropic formulations [8], [10]. An effort has been made in this paper to develop a material model which combines the model according to Chaboche and isotropic yield surface according to von Mises or anisotropic yield surface according to Hill. An anisotropic damage model according to Chaboche has also been integrated to study the damage in the post-elastic phase [6], [10].

2 Experimental Basis for Validation

In order to describe the properties of the weld in a FE model that can cover all the possible impact loads, sheet thicknesses, types of loading etc., robust material models are required. To characterize the weld and its surrounding areas, there are 3 different types of test cases with a single weld joining the top and bottom flanges. Fig. 1a shows a simple lap shear specimen where the shear forces across the weld are dominant. Fig. 1b shows a tensile-shear specimen (KS2) under different load angles. During real crash, one cannot define the angle or direction of impact. Therefore the KS2 coupon is subjected to different load angles like 0°, 30°, 60° and 90°. Fig. 1c shows a coach-peel specimen where the weld is subjected to normal and bending forces.

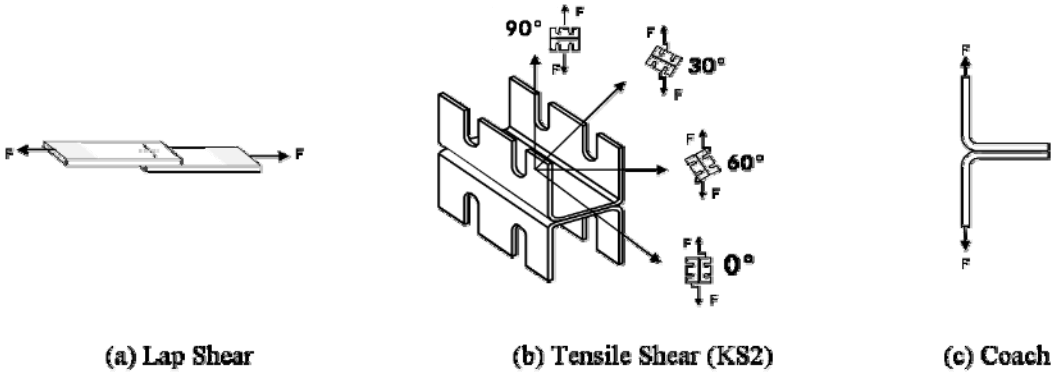

Fig. 1: Test coupons used in crash test

These coupons subjected to different loading conditions give information on the wear or tear of the weld. Hence they form the basis for designing the geometry and material of the numerical model of the

weld. The results and know-how obtained through these cases are then transferred to more complex structures like the T- Component and parts of BIW.

3 A FE Substitute Model for Laser Welded Joints

A simplified FE model which consists of the upper and lower flanges modeled with shell elements and a weld element between the flanges is called a substitute model. The element size used in the flanges is more or less the same as in the BIW target structure. Due to the fact that the crash model of a BIW target structure has a relatively coarse mesh, the FE models of the above coupons used to test the characteristics of a single weld are just made of a few elements. Fig. 2 shows a KS2 substitute model with the weld modeled as a solid.

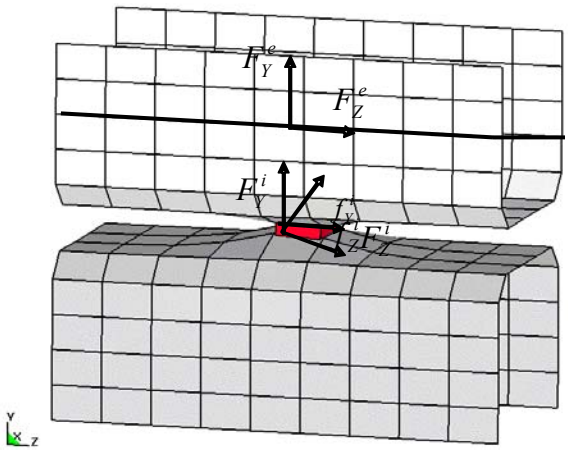

Fig. 2: A simplified FE substitute model with external and internal forces

The force is measured close to the KS2 fixation in the testing machine and the displacement is measured globally which includes the stiffness of the testing machine. Thus the force-displacement characteristic covers the overall stiffness of the testing machine and of the specimen. From the model shown in Fig. 2 the gobal forces as well as the local weld forces can be determined. The stiffness of the testing machine was modeled by beam elements on top and bottom of the specimen, where the stress-strain behavior of the beams was modeled by a load curve with the non-linear elastic material MAT_NONLINEAR_DISCRETE_BEAM [2].

In a 90° load case of KS2 specimen the flange deformations dominate the force-displacement curves, in contrast to the 0° load case of KS2 specimen where the shear deformations of the weld dominate the force-displacement response. Therefore the 0° load case and the 90° load case of KS2 specimen are used to calibrate the material behavior and determine the geometry of the weld, respectively [1].

The weld for which a new material model will be developed is the laser welded joint also known as Robscan joint [1]. Unlike the spot welds where the diameter of the spot weld is basically characterized by the sheet thickness, a single laser weld can have any shape and size depending on the desired load carrying capability.

Fig. 3: Bracket, circular and line weld

The strength of the laser weld does not only depend on the weld geometry but also on the intensity of the laser beam, the focus diameter of the beam etc. [7]. The focus diameter can vary anywhere between 0.3 mm to 0.8 mm. As a result, a laser weld has a thickness close to the focus diameter of the beam. In reality, it is approximately 1.5 times the size of the focus diameter. Some of the possible weld configurations are shown in Fig. 3.

As the BIW is discretized by a coarse mesh for flanges and welds, the above weld geometries have to be built using just a few FE elements. It consists of sheets made up of different sheet thicknesses and materials. The thickness of a sheet in a combination can typically vary from 0.6 mm to 2.5 mm. The material could be low strength steel with a maximum strength of 200 MPa or high strength steel with a tensile strength above 1000 MPa. The material model used, should be not only able to reproduce the various phases as mentioned above, but also suitable for different element types and different weld configurations. In this paper only the modeling technique with a solid element for the weld will be discussed.

4 Material Models

4.1 Linear Elastic-Visco-Plastic Model (MAT 24)

This material model also known as MAT_PIECEWISE_LINEAR_PLASTICITY or material type MAT24 [4], is a widely used material model for crash applications. It has simple yield criteria according to von Mises. Here an arbitrary elasto-plastic stress strain curve and arbitrary strain rate can be defined. By defining a tangent modulus a bi-linear stress strain behavior can be induced or effective stress to effective plastic strain curves can be directly inserted in the material card. It uses the Cowper-Symonds model to scale the yield stresses to reproduce the strain rate effects [4]. This model scales the yield stress with a factor $1+\left(\frac{\dot{\varepsilon}}{C}\right)^{\frac{1}{P}}$, where $\dot{\varepsilon}=\sqrt{\dot{\varepsilon}_{ij}\dot{\varepsilon}_{ij}}$ [4] are the strain rates, P and C are strain rate parameters. For visco-plastic formulation the following equation is employed

$$\sigma_y(\varepsilon_{eff}^P,\dot{\varepsilon}_{eff}^P)=\sigma_y^S\left(\varepsilon_{eff}^P\right)+SIGY\left(\frac{\dot{\varepsilon}_{eff}^P}{C}\right)^{\frac{1}{P}}. \quad (1)$$

Here ε_{eff}^P and $\dot{\varepsilon}_{eff}^P$ are effective plastic strain and effective plastic strain rates, respectively, while σ_y, σ_y^S and $SIGY$ are dynamic yield stress, static yield stress and initial yield stress, respectively.

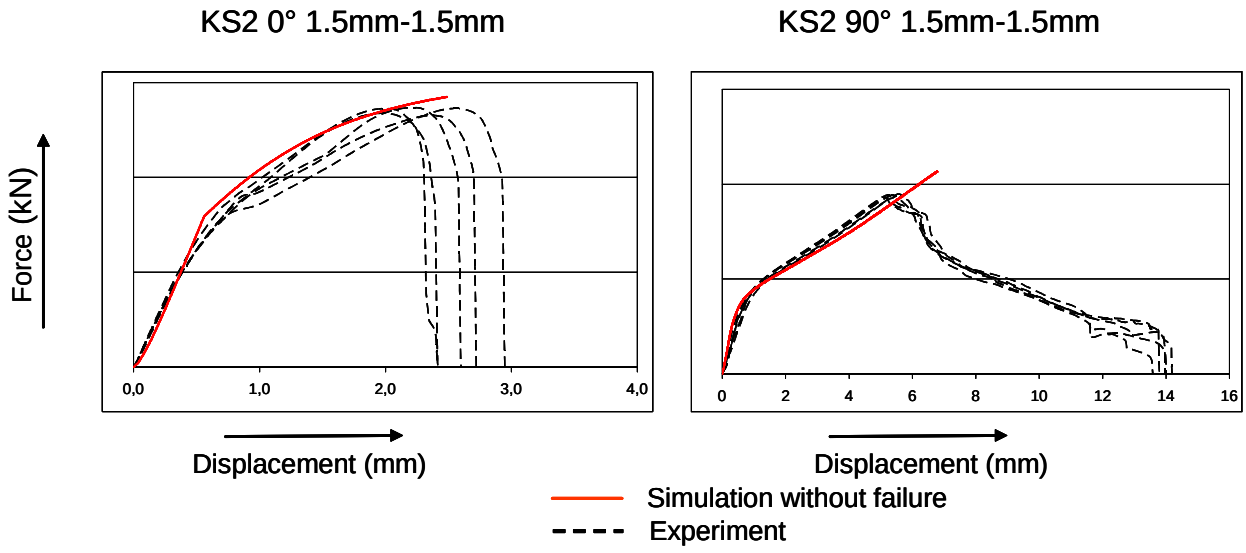

Fig. 4: Comparison of force-displacement curves using MAT24

Fig. 4 shows the comparison of experimental and simulated force-displacement curves for KS2 coupons subjected to shear and normal loads for a 1.5 mm-1.5 mm gage combination for H320LA sheets. The simulated force-displacement curves show excellent correlation with the experimental curve.

This material model can be used when strain effects play an important role. Here the material curves can be directly given as an input in the material card and can be used for almost all kinds of elements in LS-DYNA. However, it gives the possibility to write a user defined failure routine with limited options only, and it's not sufficient enough to define a proper failure criterion for crash applications. This is evident in the simulation curve in Fig. 4 where no failure in the model is observed. The model does not take material damage into account or support anisotropic flow. The importance of anisotropic flow and damage will be illustrated at a later stage in this paper.

4.2 Bi-linear Elasto-Plastic Model (MAT100)

This material model also known as MAT_SPOT_WELD or material type MAT100 [4], is a material model for modeling spot welds in crash applications [2]. This material model has a von Mises yield condition. It is linearly elastic till plasticity and upon reaching the yield condition it switches over to linear plasticity (refer Fig. 5). As input data only Young's modulus E and Poisson's ratio ν for the elastic range and the yield stress σ_y and the hardening modulus $E_{\tan}$ for the plastic range are required.

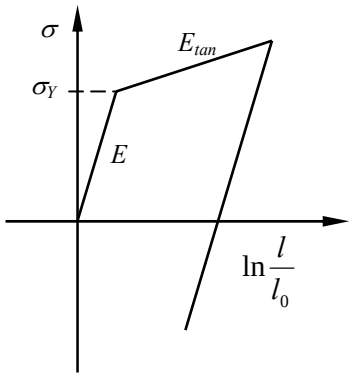

Fig. 5: Bi-linear Elasto-Plastic behavior in MAT100

Forces/moments or stresses in the spot weld are calculated in the MAT100 subroutine. On the basis of the strain increment the element stresses are calculated by the bilinear elastic-plastic material law. Since the MAT_SPOTWELD option can be only used with ELTYP=1 (reduced integration) element stresses exist only for one Gaussian point [5].

This material model has a 3-D failure criterion to describe the failure behavior of welded joints and spot welds in particular. The failure criterion describes a polynomial failure surface as shown in Fig. 6. Eqn. (2) shows the failure criterion where internal normal, bending and shear stresses are included to characterize the failure:

$$f_{3D} = \left(\frac{\sigma_N}{S_N}\right)^{n_S} + \left(\frac{\sigma_B}{S_B}\right)^{n_B} + \left(\frac{\tau}{S_S}\right)^{n_N} < 1. \qquad (2)$$

If dynamic effects in the form of strain rate sensitivity are included, the failure criterion reads

$$f_{3D} = \left(\frac{\sigma_N(\dot{\varepsilon})}{S_N(\dot{\varepsilon})}\right)^{n_S} + \left(\frac{\sigma_B(\dot{\varepsilon})}{S_B(\dot{\varepsilon})}\right)^{n_B} + \left(\frac{\tau(\dot{\varepsilon})}{S_S(\dot{\varepsilon})}\right)^{n_N} < 1, \qquad (3)$$

where

$S_N(\dot{\varepsilon}) = \overline{S}_N\, f_N(\dot{\varepsilon}),\ S_B(\dot{\varepsilon}) = \overline{S}_B\, f_B(\dot{\varepsilon})$ and $S_S(\dot{\varepsilon}) = \overline{S}_S\, f_S(\dot{\varepsilon}).$

The strain rate functions $f_N(\dot{\varepsilon}),\ f_B(\dot{\varepsilon})$ and $f_S(\dot{\varepsilon})$ are defined by load curves.

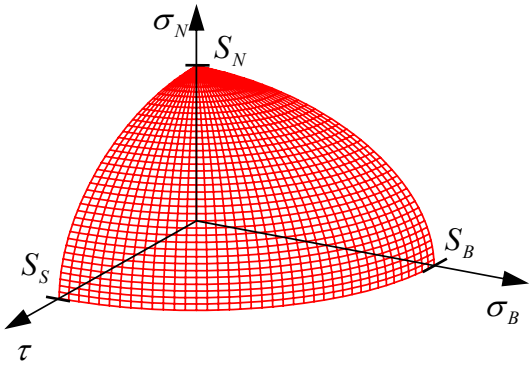

Fig. 6: 3-D failure surface - according to normal, bending and shear stress [2]

Fig. 7 shows the comparison of experimental and simulated force-displacement curves for KS2 coupons subjected to shear and normal loads for a 1.5 mm-1.5 mm gage combination for H320LA material. Though the results are good for quasi static applications, this particular material model is tailor-made for spot weld models and it may not be possible to describe the failure modes of complex Robscan joints (refer Fig. 3) where the weld orientation, the length of the Robscan weld etc. play an important role. A strain based failure criteria could be more applicable to Robscan joints which has varying geometries. Mat100 has a stress based failure criteria as described in Eqns. (2) and (3).

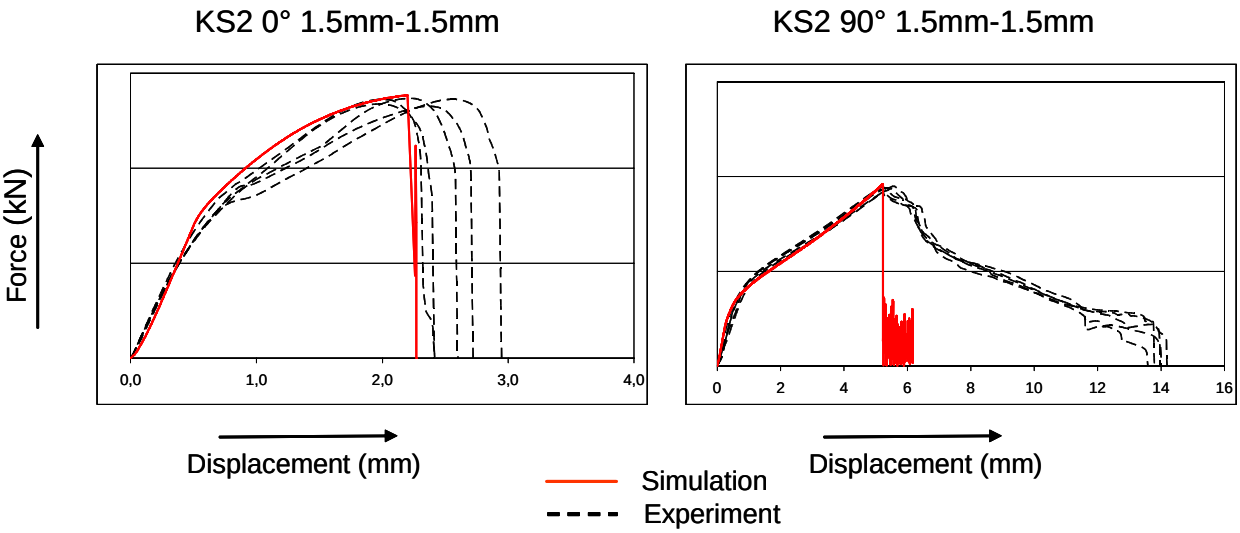

Fig. 7: Comparison of force-displacement curves using MAT 100

4.3 Material Model According to Hill and Chaboche

In this material model newly developed at Research Technology, DaimlerChrysler AG, effort has been made to answer the pit falls of the above mentioned models. The model itself has evolved through several stages of development depending on the need to answer the problems related to laser welded joints in crash.

4.3.1 Elasto-visco-plastic formulation coupled with isotropic damage:

In this particular case, a linear elastic and non-linear visco-plastic formulation according to Chaboche [8] has been used. This visco-plastic formulation can be combined with either von Mises isotropic yield condition or with a more complex anisotropic yield condition according to Hill. Material models with isotropic yield condition are generally suitable for all structures and components made of steel.

However, for some special applications such as laser welded joints where yielding is not homogenous due to structural and material influences, an anisotropic yield condition is best suitable.

In general, the total strain rate at any point of loading comprises of elastic and inelastic parts. For small deformations the total strain rate $\dot{\varepsilon}_{ij}$ can be expressed as an additive decomposition of elastic $\dot{\varepsilon}_{ij}^{e}$ and inelastic $\dot{\varepsilon}_{ij}^{P}$ strain rates as

$$\dot{\varepsilon}_{ij} = \dot{\varepsilon}_{ij}^{e} + \dot{\varepsilon}_{ij}^{P}. \tag{4}$$

The stress increment can be calculated from Hooke's law. Here the plastic strain rate is calculated according to the Chaboche model and then the elastic strain rate is determined from the total strain rate, so that

$$\dot{\sigma}_{ij} = C_{ijkl}(\dot{\varepsilon}_{kl} - \dot{\varepsilon}_{kl}^{P}), \tag{5}$$

where $\dot{\sigma}_{ij}$ and C_{ijkl} are stress increments and material tensor, respectively. Just as in most of the material models, it is important to employ a yield condition to check whether plasticity has been reached. Different yield conditions can be coupled with plasticity theory according to Chaboche. Hill's form of anisotropic yield condition is combined with the Chaboche model in this paper. By careful choice of coefficients in Hill's criterion, the von Mises criterion can also be obtained as a special case. A general formulation for Hill's anisotropic flow condition is given by

$$F(\sigma_{11} - \sigma_{22})^2 + G(\sigma_{22} - \sigma_{33})^2 + H(\sigma_{33} - \sigma_{11})^2 + 2I\sigma_{12}{}^2 + 2J\sigma_{23}{}^2 + 2K\sigma_{13}{}^2 = 1. \tag{6}$$

If X, Y, Z are uniaxial yield stresses and R, S, T are yield stresses in pure shear then the coefficients F, G, H, I, J and K are represented as follows

$$F = \frac{1}{2}\left(\frac{1}{Y^2} + \frac{1}{Z^2} - \frac{1}{X^2}\right),\ G = \frac{1}{2}\left(\frac{1}{Z^2} + \frac{1}{X^2} - \frac{1}{Y^2}\right),\ H = \frac{1}{2}\left(\frac{1}{Y^2} + \frac{1}{X^2} - \frac{1}{Z^2}\right),$$

$$I = \frac{1}{2R^2},\ J = \frac{1}{2S^2},\ K = \frac{1}{2T^2}.$$

By introducing a tensor function of the 4th order $\mathbf{M}$ (see [9]), the anisotropic yield criterion can be generalized as follows

$$F(\boldsymbol{\sigma}, \mathbf{M}) = F(\sigma_{ij}, M_{ijkl}) = 0, \tag{7}$$

where the 4th order tensor M_{ijkl} takes the form

$$M_{ijkl} = \begin{bmatrix} M_{1111} & M_{1122} & M_{1133} & & & \\ & M_{2222} & M_{2233} & & 0 & \\ & & M_{3333} & & & \\ & & & M_{1212} & & \\ & symm. & & & M_{2323} & \\ & & & & & M_{3131} \end{bmatrix}$$

with

$$M_{1111} = F + H,\ M_{2222} = F + G,\ M_{3333} = G + H,\ M_{1122} = -F, M_{2233} = -G,\ M_{3311} = -H,$$
$$M_{3131} = \frac{1}{2}K,\ M_{2323} = \frac{1}{2}J,\ M_{1212} = \frac{1}{2}I.$$

By letting $I = J = K = 3F = 3G = 3H$, the von Mises criterion can be recovered from Eqn. (6). Then the 4th order tensor $\hat{\mathbf{M}}$ will have the following coefficients, where σ_y denotes the yield stress:

$$\hat{\mathbf{M}} = \frac{1}{\sigma_y^2}\begin{bmatrix} 1 & -\frac{1}{2} & -\frac{1}{2} & & & \\ & 1 & -\frac{1}{2} & & 0 & \\ & & 1 & & & \\ & & & \frac{3}{2} & & \\ & \textit{symm.} & & & \frac{3}{2} & \\ & & & & & \frac{3}{2} \end{bmatrix}. \qquad (8)$$

Fig. 8 shows a general comparison of the Hill and von Mises yield surfaces. As in the characteristic equation according to Hill (Eqn. 6), Hill's yield surface is an ellipse with σ_1, σ_2 as nominal stresses and σ_s as plastic threshold.

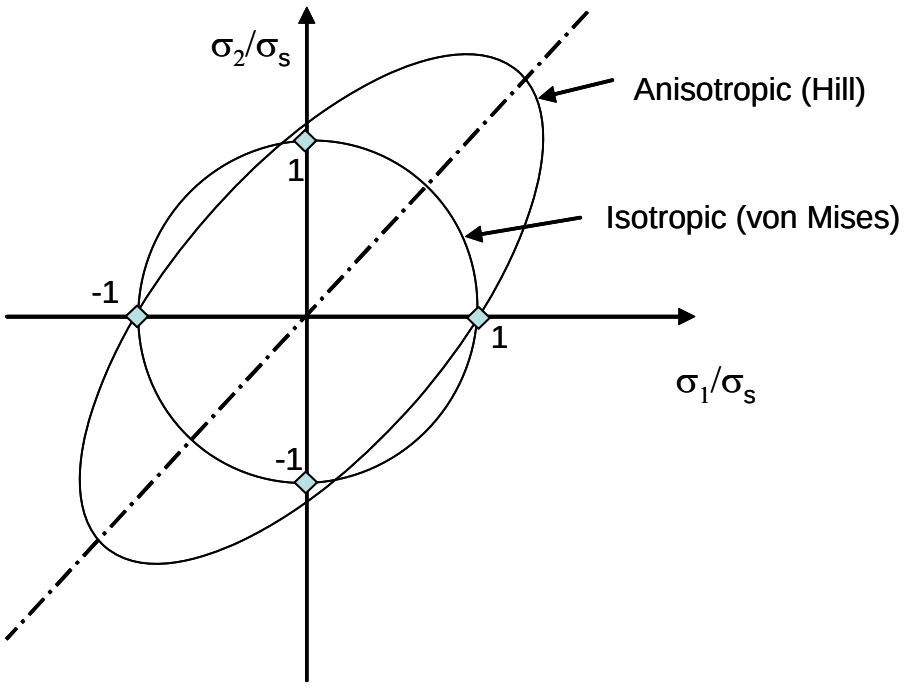

Fig. 8: Comparison of Hill and von Mises yield surfaces

The dissipation potential expressed as a function of associated thermodynamic variables and dependent state variables can be generally written as $\varphi^* = \Omega(\boldsymbol{\sigma}, \mathbf{X})$. $\mathbf{X}$ describes the backstress or non-linear kinematic hardening tensor. The dissipation potential can be expressed as a function of elementary invariants of $\boldsymbol{\sigma} - \mathbf{X}$, $\mathbf{X}$ and $\boldsymbol{\sigma}$. For our application, the effect of the third invariant is ignored. The dissipation potential will then take the form

$$\Omega = \Omega(J_M(\boldsymbol{\sigma} - \mathbf{X}), J_M(\mathbf{X}); J_M(\boldsymbol{\alpha})), \tag{9}$$

where $\boldsymbol{\alpha}$ is a kinematic hardening parameter. $J_M()$ is a stress norm according to Hill comparable to the second invariant $J_2()$ with

$$J_M(\boldsymbol{\sigma} - \mathbf{X}) = \left[(\boldsymbol{\sigma}' - \mathbf{X}') : \mathbf{M} : (\boldsymbol{\sigma}' - \mathbf{X}')\right], \tag{10}$$

where $\boldsymbol{\sigma}'$ and $\mathbf{X}'$ are normal deviatoric stresses and deviatoric back stresses, respectively.

If the Hill criterion is reduced to the von Mises criterion by replacing $\mathbf{M}$ with $\hat{\mathbf{M}}$ in Eqn (10), then the stress norm $J_2()$ according to von Mises will take the form

$$J_2(\boldsymbol{\sigma} - \mathbf{X}) = \left[\frac{3}{2}(\boldsymbol{\sigma}' - \mathbf{X}') : (\boldsymbol{\sigma}' - \mathbf{X}')\right]. \tag{11}$$

The non-linear kinematic hardening which was initially developed by Armstrong and Frederick (see [8]) for time dependent plasticity and later expanded for visco-plasticity by Malinin and Khadjinsky (see [8]) is based on an evolution equation in $\mathbf{X}$ containing a linear kinematic hardening term and a recall term to provide fading memory effect along the deformation path as shown in Eqn. (11). This equation gives the kinematic strain rate for isotropic yield condition

$$\dot{X}_{ij} = \frac{2}{3} a \dot{\varepsilon}^P_{ij} - s X_{ij} \dot{P}. \tag{12}$$

Here a and s are material parameters and $\dot{P}$ is the equivalent plastic strain rate according to Chaboche. Eqn. (12) is homogeneous with the first term and therefore the effect of recall is time and rate independent, which means that the model represents non-linear strain hardening without effect of recovery with time. Therefore within the general thermodynamic framework it is necessary to keep $\boldsymbol{\alpha}$ in the dissipation potential equation. Hence Eqn. (9) can be rewritten as

$$\Omega = \Omega(J_2(\boldsymbol{\sigma} - \mathbf{X}) - \kappa + \frac{s}{2a} + J_2(\mathbf{X}) - \frac{2sa}{9} J_2^2(\boldsymbol{\alpha})) \tag{13}$$

where the coefficients a, s are material constants and κ the yield stress of the material.

Eqn. (13) can be generalized for anisotropic yield condition as follows

$$\Omega = \Omega(J_M(\boldsymbol{\sigma} - \mathbf{X}) - \tilde{\kappa} + \frac{s}{2a} + J_M(\mathbf{X}) - \frac{2sa}{9} J_M^2(\boldsymbol{\alpha})) \tag{14}$$

where $\tilde{\kappa}$ is a yield stress.

The visco-plastic strain rate $\dot{\varepsilon}_P$ according to Chaboche can be derived from the dissipation potential Ω as

$$\dot{\varepsilon}_p = \frac{\partial \Omega}{\partial \sigma} = \frac{\partial \Omega}{\partial J_M} \frac{\partial J_M}{\partial \sigma}$$

With

$$\frac{\partial J_M}{\partial \sigma} = \frac{\partial}{\partial \sigma} \sqrt{(\boldsymbol{\sigma}' - \mathbf{X}') : \mathbf{M} : (\boldsymbol{\sigma}' - \mathbf{X}')} \ , \ \frac{\partial \Omega}{\partial J_M} = \dot{P}$$

we get

$$\dot{\varepsilon}_p = \frac{\mathbf{M} : (\boldsymbol{\sigma}' - \mathbf{X}')}{J_M (\boldsymbol{\sigma} - \mathbf{X})} \dot{P} \tag{15}$$

or

$$\dot{\varepsilon}_p = \frac{3(\boldsymbol{\sigma}' - \mathbf{X}')}{2J_2 (\boldsymbol{\sigma} - \mathbf{X})} \dot{P} \tag{16}$$

for isotropic flow condition.

A general form of the free energy ψ is assumed to include a quadratic term in $\boldsymbol{\alpha}$ [8] and expressed as

$$\begin{aligned} \rho\psi &= \rho\psi_e + \frac{2}{9} a J_M^2 (\boldsymbol{\alpha}) \\ &= \rho\psi_e + \frac{2}{9} a \boldsymbol{\alpha} : \mathbf{M} : \boldsymbol{\alpha} \end{aligned}$$

where ψ_e is the specific internal free energy and ρ denotes the density.

The back stress $\mathbf{X}$ and consequently the back stress rate $\dot{\mathbf{X}}$ can be obtained from the free energy as

$$\begin{aligned} \mathbf{X} &= \rho \left(\frac{\partial \psi}{\partial \alpha} \right) \\ &= \frac{\partial}{\partial \alpha} \left(\frac{2}{9} a \boldsymbol{\alpha} : \mathbf{M} : \boldsymbol{\alpha} \right). \end{aligned}$$

The back stress rate can be derived by a time derivative as

$$\dot{\mathbf{X}} = \frac{4}{9} a \mathbf{M} : \dot{\boldsymbol{\alpha}} . \tag{17}$$

The rate of kinematic hardening parameter $\dot{\boldsymbol{\alpha}}$ can be obtained from the dissipation potential as

$$\dot{\boldsymbol{\alpha}} = -\frac{\partial \Omega}{\partial \mathbf{X}} = \dot{\boldsymbol{\varepsilon}}_\mathbf{p} - \frac{a}{s} \mathbf{M} : \mathbf{X} \dot{P} . \tag{18}$$

By combining Eqn. (17) and Eqn. (18), the kinematic back stress rate can be obtained with the anisotropic Matrix $\mathbf{M}$ as

$$\dot{\mathbf{X}} = \frac{4}{9} a\, \mathbf{M} : \dot{\boldsymbol{\varepsilon}}_{\mathbf{p}} - \frac{4}{9} s\, \dot{P}\, \mathbf{M} : [\mathbf{M} : \mathbf{X}] . \tag{19}$$

For an isotropic yield condition, Eqn. (19) can be reduced to the form as in Eqn. (12).

Finally the dissipation potential Ω can be expressed as a power function [8]

$$\Omega = \frac{K}{n+1} \left\langle \frac{J_M(\boldsymbol{\sigma} - \mathbf{X}) - \tilde{\kappa}}{K} \right\rangle^{n+1}, \tag{20}$$

where K and n are material parameters and $\langle\rangle$ is the Mc Cauley bracket with $\langle x \rangle = \frac{1}{2}(x + |x|)$. Before reaching plasticity, $J_M(\boldsymbol{\sigma} - \mathbf{X}) - \tilde{\kappa}$ has a negative value and the value within the Mc Cauley bracket is zero.

The equivalent plastic strain rate $\dot{P}$ according to Chaboche used in the equations above can be deduced from Eqn. (20).

With $\dot{P} = \frac{\partial \Omega}{\partial J_M}$ we get

$$\dot{P} = \left\langle \frac{J_M(\boldsymbol{\sigma} - \mathbf{X}) - \tilde{\kappa}}{K} \right\rangle^{n} = \left\langle \frac{\sigma_{eq}}{K} \right\rangle^{n} . \tag{21}$$

As far as the work in this paper is concerned only small deformations are considered. As mentioned before there are a number of damage models which can be coupled with plasticity and are strongly dependent on the type of application. Some of the known damage models are ductile plastic damage, creep damage, fatigue damage etc. As far as the scope of the paper goes, only ductile plastic damage is considered. If only isotropic damage and hardening are considered, the one and only one internal variable that appears, besides damage, is the accumulated plastic strain. Starting from the dissipation potential φ_D^*, which includes damage as an internal variable, a multi-axial strain based model can be developed in the form of

$$\dot{D} = \frac{D_c}{\varepsilon_R - \varepsilon_D} \left[\frac{2}{3}(1+\nu) + 3(1-2\nu) \left(\frac{\sigma_h}{\sigma_{vM}} \right)^2 \right] \dot{P}, \tag{22}$$

where $\dot{D}$ is the damage rate, D_c is the critical damage parameter, ε_R the strain at rupture and ε_D the damage threshold strain. The parameter ε_D controls the initiation of damage. If this damage variable is set to zero, damage starts upon reaching plasticity. As the damage model is controlled by equivalent plastic strain rate, this model is also called as the plastic damage model. For a uniaxial tensile condition the triaxiality function $\frac{2}{3}(1+\nu) + 3(1-2\nu)\left(\frac{\sigma_h}{\sigma_{vM}} \right)^2$ yields a value equal to unity. Here ν is the elastic Poisson's ratio which is approx. 0.33 for metals and σ_H and σ_{vM} are the hydrostatic stress and von Mises equivalent stress, respectively.

If isotropic damage is used, then the modulus of elasticity and the effective anisotropic stress need to be suitably changed. Firstly,

$$\tilde{E} = E(1-D),$$

where $\tilde{E}$ is the newly calculated elasticity modulus and D the accumulated damage. And secondly

$$\tilde{J}_M(\boldsymbol{\sigma}-\mathbf{X}) = J_M\left(\frac{\boldsymbol{\sigma}-\mathbf{X}}{1-D}\right),$$

where $\tilde{J}_M()$ is the effective anisotropic stress with damage.

4.3.2 Elasto-visco-plastic formulation coupled with anisotropic damage and weld failure criterion:

A suitable anisotropic damage model can be realized if $\dot{P}$ is replaced by the plastic strain rate $\dot{\varepsilon}_{ij}^{P}$ [6] in Eqn. (22). As the strain rates can be negative, the absolute value is considered to calculate the damage rate and its subsequent damage accumulation

$$\dot{D}_{ij} = \frac{D_c}{\varepsilon_R - \varepsilon_D}\left[\frac{2}{3}(1+\nu) + 3(1-2\nu)\left(\frac{\sigma_h}{\tilde{\sigma}_{vM}}\right)^2\right]|\,\varepsilon_{ij}^{P}\,|. \tag{24}$$

By introducing anisotropic damage, effective stresses in the material need to be recalculated. The new effective stress and von Mises stress can be calculated as follows

$$\tilde{\sigma}_{ij} = H_{ik}\sigma'_{kl}H_{lj} + \frac{\sigma_H}{1-\lambda D_H}\delta_{ij}, \tag{25}$$

$$\tilde{\sigma}_{vM} = H_{ik}\tilde{\sigma}_{kl}H_{lj},$$

where $H_{ij} = (\delta_{ij} - D_{ij})^{-\left(\frac{1}{2}\right)}$, δ_{ij} denotes the Kronecker symbol and σ'_{kl} is the deviatoric stress. Furthermore λ is a parameter used for correct representation of experiments concerning variations in Poisson's ratio [10]. It is purely material dependent and characterizes the effect of hydrostatic stresses. For most of metals λ is approx. 3. D_H is the mean damage equal to $\frac{1}{3}D_{kk}$.

By using the concept of effective stress as in Eqn. (25) and the formulation of H_{ij} for anisotropic damage, the stress norm according to Hill, the plastic strain rate and the back stress rate can be modified as shown in Eqns. (26), (27) and (28), respectively.

$$J_M\left(\mathbf{H}\left[\boldsymbol{\sigma}-\mathbf{X}\right]\mathbf{H}\right) = \mathbf{H}\left[\boldsymbol{\sigma}'-\mathbf{X}'\right]\mathbf{H} : \mathbf{M} : \mathbf{H}\left[\boldsymbol{\sigma}'-\mathbf{X}'\right]\mathbf{H}, \tag{26}$$

$$\dot{\varepsilon}_p = \frac{\mathbf{M} : \mathbf{H}\left[\tilde{\boldsymbol{\sigma}}'-\mathbf{X}'\right]\mathbf{H}}{J_M\left(\mathbf{H}\left[\tilde{\boldsymbol{\sigma}}-\mathbf{X}\right]\mathbf{H}\right)}\dot{P}, \tag{27}$$

$$\dot{\mathbf{X}} = a\frac{(\tilde{\boldsymbol{\sigma}}' - \mathbf{X}')}{J_M\left(\mathbf{H}[\tilde{\boldsymbol{\sigma}} - \mathbf{X}]\mathbf{H}\right)}\dot{P} - s\mathbf{X}\frac{J_M(\boldsymbol{\sigma} - \mathbf{X})}{J_M\left(\mathbf{H}[\tilde{\boldsymbol{\sigma}} - \mathbf{X}]\mathbf{H}\right)}\dot{P}\,. \tag{28}$$

Until Eqn. (28), a general elasto-visco-plastic formulation with anisotropic damage has been presented. As mentioned earlier, for laser welded joints, the failure of the weld for different loading cases is a complex phenomenon. The nature of weld failure depends on the type of loading which is demonstrated in Fig. 9.

"Weld tear off" in a KS2 0° 1.5mm-1.5mm gauge combination

"Pull out failure" in a KS2 90° 1.5mm-1.5mm gauge combination

Fig. 9: Comparison of weld failures for different loading cases

In a KS2 0° loading case the shear forces dominate around the weld resulting in a weld tear off. In a KS2 90° loading case, normal forces act around the weld pulling the weld away from the flanges. Generally in this case the failure occurs in the heat affected zone.

Effort has been made in this paper to describe this failure in the form of a simple equation. Eqn. (29) shows a simple failure criterion generated from anisotropic damage evolution and the anisotropic yield matrix

$$\mathbf{D} : \mathbf{M} : \mathbf{D} \geq D_{\max}\,. \tag{29}$$

Where $D_{\max}$ is the maximum permissible damage for a weld geometry resulting from a particular material combination. In other words, the failure of the weld takes place for any loading case when $D_{\max}$ is reached. In order to achieve this, the flow stresses X, Y, Z and R, S and T can be adjusted accordingly. This is one of the main advantages of this newly developed material model according to Hill and Chaboche.

Fig. 10 shows the comparison of experimental and simulated force-displacement curves for KS2 coupons subjected to shear and normal loads for a 1.5 mm-1.5 mm gage combination for H320LA material. It shows a good agreement of force-displacement curves until the maximum load. As far as crash is concerned the behavior of the weld until the maximum load is of relevance. If an anisotropic yield condition is not implemented, failure does not take place in a KS2 90° loading case. In this particular case the bending of the flanges actually dominate the weld deformation. But in order to

create a failure in a substitute weld model, by reducing the flow stress in the direction of loading in a KS2 90° loading case, a faster accumulation of plastic damage is made possible.

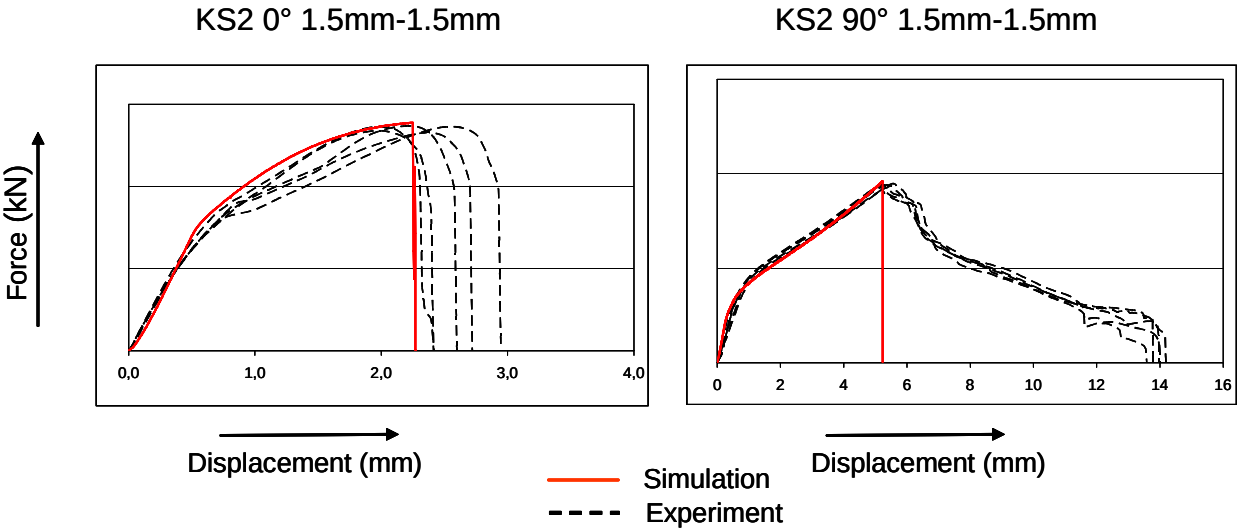

Fig. 10: Comparison of force-displacement curves using the new material model according to Hill and Chaboche

5 Conclusions

The newly developed material model according to Hill and Chaboche is a complex material model capable of demonstrating all the phases from simple elasticity to visco-plasticity with an anisotropic yield surface. Anisotropic damage formulation has also been incorporated. This model has been further developed to suit the crash application by introducing a simple failure criterion. The model together with the failure criterion has been tested on coupons subjected to different loading cases. Depending on the results, it may be required to alter the anisotropic yield matrix $\mathbf{M}$ as in Eqn. (29) to a weighting matrix for anisotropic failure. It has to be further tested on other specimens where not only shear and normal forces act but also the bending forces. After successful implementation at the coupon level it will be tested on components and BIW. This material model which can be used for any structures or parts made of steel may also find its application where anisotropic yield surface and anisotropic damage play an important role.

References

[1] Kuppuswamy, N., Schmidt, R., Seeger, F., Zhang, S.: Finite Element Modeling of Impact Strength of Laser Welds for Automotive Applications, High Performance Structures and Materials III, Ostend, Belgium 2006, WIT Press, Southampton, UK, in print

[2] Seeger, F., Feucht, M., Frank, Th., Keding, B., Haufe, A.: An Investigation on Spot Weld Modeling for Crash Simulation with LS-DYNA, 4. LS-DYNA User Conference, Bamberg 2005

[3] Stoffel, M.: Non-linear Dynamics of Plates, PhD Thesis, Institute of General Mechanics, RWTH Aachen, November 2000

[4] LS DYNA Non-linear Analysis of Structures, User's Manual, Livermore Software Technology Cooperation, Livermore, California 2005

[5] LS DYNA Theoretical Manual, Livermore Software Technology Cooperation, Livermore, California, May 1998

[6] Stoffel, M., Schmidt, R., Weichert, D.: Anisotropic Damage of Shock Wave- Loaded Plates, GAMM 2006, TU Berlin, 27th-31st March 2006, PAMM, in print

[7] Hopf, B.: Significance of Laser Technology in Production, Production and Materials Technology, DaimlerChrysler HighTechReport, February 2004

[8] Lemaitre, J., Chaboche, J. L.: Mechanics of Solid Materials, Cambridge Press, 1998

[9] Khan, A.S., Huang, S.: Continuum Theory of Plasticity, John Wiley & Sons, Inc, 1995

[10] Lemaitre, J., Desmorat, R., Sauzay, M.: Anisotropic Damage Law of Evolution, Eur. J. Mech. A/Solids 19 (2000) 187-208

